

The surviving companions in type Ia supernova remnants

Li-Qing Chen^{1,2,3}, Xiang-Cun Meng^{1,2,4} and Zhan-Wen Han^{1,2,4}

¹ Yunnan Observatories, Chinese Academy of Sciences, Kunming 650216, China; liqingch@ynao.ac.cn

² Key Laboratory for the Structure and Evolution of Celestial Objects, Chinese Academy of Sciences, Kunming 650216, China

³ University of Chinese Academy of Sciences, Beijing 100049, China

⁴ Center for Astronomical Mega-Science, Chinese Academy of Sciences, Beijing 100012, China

Received 2017 February 22; accepted 2017 April 27

Abstract The single-degenerate (SD) model is one of the most popular progenitor models of type Ia supernovae (SNe Ia), in which the companion star can survive after an SN Ia explosion and show peculiar properties. Therefore, searching for the surviving companion in type Ia supernova remnants (SNRs) is a potential method to verify the SD model. In the SN 1604 remnant (Kepler's SNR), although Chandra X-ray observation suggests that the progenitor is most likely a WD+AGB system, the surviving companion has not been found. One possible reason is rapid rotation of the white dwarf (WD), causing explosion of the WD to be delayed for a spin-down timescale, and then the companion evolved into a WD before the supernova explosion, so the companion is too dim to be detected. We aim to verify this possible explanation by carrying out binary evolution calculations. In this paper, we use Eggleton's stellar evolution code to calculate the evolution of binaries consisting of a WD+red giant (RG). We assume that the rapidly rotating WD can continuously increase its mass when its mass exceeds the Chandrasekhar mass limit ($M_{\text{Ch}} = 1.378 M_{\odot}$) until the mass-transfer rate decreases to be lower than a critical value. Eventually, we obtain the final masses of a WD in the range $1.378 M_{\odot}$ to $2.707 M_{\odot}$. We also show that if the spin-down time is less than 10^6 yr, the companion star will be very bright and easily observed; but if the spin-down time is as long as $\sim 10^7$ yr, the luminosities of the surviving companion would be lower than the detection limit. Our simulation provides guidance in hunting for the surviving companion stars in SNRs, and the fact that no surviving companion has been found in Kepler's SNR may not be definite evidence disfavoring the SD origin of Kepler's SN.

Key words: stars: evolution — binaries: symbiotic — supernovae: individual (SN 1604, SN 1006)

1 INTRODUCTION

Type Ia supernovae (SNe Ia) are used as cosmologic distance indicators due to the homogeneity of their properties, and thus are applied to determine cosmological parameters (e.g. Ω and Λ ; Riess et al. 1998; Perlmutter et al. 1999). This approach enabled the discovery of accelerated expansion of the universe, and thus inferred the existence of dark energy. In addition, SNe Ia also play a key role in galactic chemical evolution owing to them being the main production sites of iron group elements (e.g. Greggio & Renzini 1983; Matteucci & Greggio 1986). However, the exact natures of the progenitors of SNe Ia are still unclear, and no progenitor system before

an SN explosion has been conclusively identified. This may directly affect the reliability of results of the current cosmological model and the galactic chemical evolution model (Wang & Han 2012; Meng et al. 2015).

It is widely accepted that SNe Ia arise from the thermonuclear explosion of carbon-oxygen white dwarfs (CO WDs) in close binaries (Nomoto et al. 1997). The most popular progenitor models are the single-degenerate (SD) model and the double-degenerate (DD) model. In the SD model, a CO WD accretes materials from a main-sequence (MS) star or subgiant star (WD+MS) channel, or a red-giant (RG) star (WD+RG channel) or a helium star (WD+He star channel), which increases its mass to M_{Ch} , and then explodes as an

SN Ia (Nomoto 1982; Hachisu et al. 1996, 1999b,a; Li & van den Heuvel 1997; Langer et al. 2000; Han & Podsiadlowski 2004; Chen & Li 2007, 2009; Meng et al. 2009; Wang & Han 2009, 2010b). In the DD model, an SN Ia arises from the merging of two close CO WDs whose total mass is above or equal to M_{Ch} (Iben & Tutukov 1984; Webbink 1984). The companion can survive after the SN Ia explosion in the SD model and potentially be identifiable due to its distinguishing properties (e.g. Wang & Han 2009, 2010a; Pan et al. 2014), but no surviving companion is expected from the DD model. Thus, searching for the surviving donor star in an SNR is a potential method to verify the SD model.

SN 1572 (Tycho Brahe’s supernova), together with SN 1006, SN 1604 (Kepler’s supernova) and the recently identified SN 185, are four known historical Galactic SNe Ia events (González Hernández et al. 2012; González-Hernández et al. 2015). Currently only three remnants have been spectroscopically searched for donor stars (SN 1572, SN 1006 and SN 1604) (Kerzendorf et al. 2012, 2013, 2014). Ruiz-Lapuente et al. (2004) investigated SN 1572 and found one promising candidate (called Tycho G) that could be the surviving companion of the progenitor of SN 1572. González Hernández et al. (2009) studied star Tycho G and obtained its stellar parameters and chemical abundances, and they found that a slight Ni enhancement was seen in Tycho G, which may imply Ni pollution from SN 1572 ejecta (e.g. González-Hernández et al. 2015). Therefore, González-Hernández et al. (2015) thought that Tycho G was possibly the only viable candidate for the surviving companion of SN 1572, but this conclusion is still being questioned (e.g. Kerzendorf et al. 2013). As for SN 1006, it is the brightest observed stellar event in recorded history, reaching an estimated apparent magnitude of -7.5 and exceeding roughly 16 times the brightness of Venus. However, no surviving companion consistent with the SD model has been found in the remnant of SN 1006 (Kerzendorf et al. 2012). Compared to SN 1572 and SN 1006, Kepler’s SNR (SNR 1604) shows a very peculiar structure which is probably derived from the interaction between supernova ejecta and circumstellar material (Kerzendorf et al. 2014; Patnaude et al. 2012). Chiotellis et al. (2012, 2013) suggested a model to describe Kepler’s SNR and found that Kepler’s SNR is consistent with a symbiotic binary progenitor composed of a WD and an AGB star (see also Burkey et al. 2013; Meng & Han 2016). Kerzendorf et al. (2014) searched for the possible surviving companion star in Kepler’s SNR. However, the results showed that there seemed to be no a viable giant donor located in SN 1604, which

contradicts the AGB model suggested by Chiotellis et al. (2012) and Burkey et al. (2013).

One possible explanation is from the spin-up/spin-down model in which the WD may increase its mass continuously when its mass exceeds the Chandrasekhar mass limit due to rapid rotation, and then the explosion of the WD is significantly delayed and the companion evolves to become too dim to detect due to its long spin-down timescale (Di Stefano et al. 2011; Justham 2011). The spin-down time is defined as the time between the end of the mass growth of the WD and the explosion. At present, however, the spin-down time is quite uncertain, from $< 10^6$ yr to $> 10^9$ yr (Lindblom 1999; Yoon & Langer 2005; Di Stefano et al. 2011). Recently Meng & Podsiadlowski (2013) used an empirical method to constrain the spin-down timescale and found that the upper limit of the spin-down timescale is a few 10^7 yr. The spin-down timescale of a few 10^7 yr is long enough to erase the predicted signature from the SD model, but it may be neglected compared with the delay time of an SN Ia. Therefore, in our work, we plan to verify this possible explanation by carrying out binary evolution calculations in detail and to verify whether the explanation may explain the non-detection result of Kepler’s companion.

In this paper, we carry out evolutionary calculations of white dwarf binaries with RG companion stars. After the mass of the WD stops growing, we follow the evolution of the companion star in order to obtain its properties corresponding to different spin-down timescales (10^4 , 10^5 , ..., 10^9 yr), aiming to provide theoretical guidance in searching for surviving companions in SNRs. In Section 2 we simply describe our binary evolution model, and the results of our calculations are presented in Section 3. We discuss the results and summarize in Sections 4 and 5, respectively.

2 BINARY EVOLUTION CALCULATIONS

We use Eggleton’s stellar evolution code (Eggleton 1971, 1972, 1973) to calculate the binary evolutions. The input physics for this code have been updated over the past four decades (Han et al. 1994; Pols et al. 1995, 1998). Roche lobe overflow (RLOF) is treated within the code as described by Han et al. (2000). The ratio of mixing length to local pressure scale height, $\alpha = l/H_p$, is set to be 2.0, and the convective overshooting parameter, δ_{OV} , is 0.12, which roughly corresponds to an overshooting length of $\sim 0.25H_p$ (Pols et al. 1997; Schroder et al. 1997). We adopt solar metallicity ($Z = 0.02$), and the opacity table for metallicity is compiled by Chen & Tout (2007) from Iglesias & Rogers (1996) and Alexander & Ferguson (1994). We consider the tidally enhanced

mass-loss model which may explain many phenomena related to the evolution of a giant star in binary systems (Tout & Eggleton 1988; Chen et al. 2011). The tidally enhanced mass-loss model may effectively avoid dynamically unstable mass transfer between the WD and its RG companion, and extend the parameter space producing SNe Ia through the symbiotic channel (Chen et al. 2011; Meng & Han 2016). Here the tidally enhanced mass-loss rate from the secondary, \dot{M}_{2w} , which is modeled by Reimers' (1975) formula with an extra tidal term introduced by Tout & Eggleton (1988), is expressed as follows (see also Chen et al. 2011; Meng & Podsiadlowski 2013; Meng & Han 2016)

$$\dot{M}_{2w} = -4 \times 10^{-13} \frac{\eta(L/L_{\odot})(R/R_{\odot})}{(M_2/M_{\odot})} \times \left[1 + B_W \min\left(\frac{1}{2}, \frac{R}{R_L}\right)^6 \right] M_{\odot} \text{ yr}^{-1}, \quad (1)$$

where L and R are the luminosity and radius of the giant secondary, R_L is its Roche lobe radius, and η is Reimers' wind coefficient which is set to 0.25. Here, we set the wind enhancement parameter B_W to 10 000, which means that $|\dot{M}_{2w}|$ may be 150 times as large as Reimers' rate when the star fills more than half of its Roche lobe (Tout & Eggleton 1988; Chen et al. 2011; Meng & Podsiadlowski 2013). However, the wind enhancement parameter B_W is still not clear but is in the range 3000 to 10 000. Chen et al. (2011) discussed the effect of B_W on the parameter space leading to SNe Ia in detail, and found that the parameter space increases with B_W .

The WD may accrete part of the material lost from the giant companion, and the accretion rate can be expressed as (from Boffin & Jorissen 1988)

$$\dot{M}_{2a} = -\frac{1}{\sqrt{1-e^2}} \left(\frac{GM_{WD}}{v_w^2} \right)^2 \frac{\alpha_{acc} \dot{M}_{2w}}{2a^2(1+v_{orb}^2/v_w^2)^{\frac{3}{2}}}, \quad (2)$$

where $v_{orb} = \sqrt{G(M_2 + M_{WD})/a}$ is the orbital velocity, G is Newton's gravitational constant, a is the semi-major axis of the orbit and e is its eccentricity. We take $e = 0$ as in Chen et al. (2011). We set the accretion efficiency α_{acc} to 1.5. For simplicity, we fix the wind velocity v_w to 5 km s^{-1} for an RG and 5 km s^{-1} is a lower limit for the wind velocity (see also Chen et al. 2011). If v_w or a is small, the right-hand side of Equation (2) can be larger than $-\dot{M}_{2w}$. Therefore, we limit $\dot{M}_{2a} \leq -\dot{M}_{2w}$ (see also Chen et al. 2011; Meng & Podsiadlowski 2013). Note that both v_w and B_W are poorly known. Chen et al. (2011) and Meng & Han (2016) discussed their effects

on the parameter spaces that lead to SNe Ia. Here we set $v_w = 5 \text{ km s}^{-1}$ and $B_W = 10\,000$, which means that the parameter space for SNe Ia is an upper limit, i.e. the results here cover all possibilities resulting from the uncertainties of B_W and v_w .

Material from the RG secondary to the WD is only transferred by stellar wind accretion before RLOF so the mass-transfer rate $\dot{M}_{tr} = \dot{M}_{2a}$. During RLOF the mass is transferred through both a stream from the inner Lagrangian point and the wind, so $\dot{M}_{tr} = \dot{M}_{2a} + |\dot{M}_{2RLOF}|$, where \dot{M}_{2RLOF} is the mass-transfer rate by RLOF.

The prescription of Hachisu et al. (1999b) is adopted for the mass growth of WD by accretion of hydrogen-rich matter from its companion (for details see Han & Podsiadlowski 2004; Meng et al. 2009; Wang et al. 2014). If the mass-transfer rate $|\dot{M}_{tr}|$ is above the critical accretion rate, \dot{M}_{cr} , we assume that hydrogen burns steadily on the surface of the WD and that hydrogen-rich matter is converted into helium at the rate \dot{M}_{cr} , while unprocessed matter is lost from the system as an optically thick wind at a mass-loss rate $\dot{M}_{wind} = |\dot{M}_{tr}| - \dot{M}_{cr}$ (Hachisu et al. 1996). The critical accretion rate is

$$\dot{M}_{cr} = 5.3 \times 10^{-7} \frac{(1.7 - X)}{X} \times (M_{WD}/M_{\odot} - 0.4) M_{\odot} \text{ yr}^{-1}, \quad (3)$$

where X is the hydrogen mass fraction and M_{WD} is the mass of the WD (mass is in solar unit). When $|\dot{M}_{tr}|$ is smaller than \dot{M}_{cr} , we adopt the following assumptions.

(1) When $|\dot{M}_{tr}|$ is higher than $\frac{1}{2}\dot{M}_{cr}$, it is assumed that there is no mass loss and that the hydrogen-shell burning is steady.

(2) When $|\dot{M}_{tr}|$ is lower than $\frac{1}{2}\dot{M}_{cr}$ but higher than $\frac{1}{8}\dot{M}_{cr}$, a very weak hydrogen-shell flash is triggered but no mass is lost from the system.

(3) When $|\dot{M}_{tr}|$ is lower than $\frac{1}{8}\dot{M}_{cr}$, hydrogen-shell flashes are so strong that no mass can be accumulated on the surface of the CO WD. Then the growth rate of the CO WD \dot{M}_{WD} is given by

$$\dot{M}_{WD} = \eta_{He} \dot{M}_{He} = \eta_{He} \eta_H |\dot{M}_{tr}|, \quad (4)$$

where \dot{M}_{He} is the growth rate of the mass of the helium layer on top of the CO WD expressed as

$$\dot{M}_{He} = \eta_H |\dot{M}_{tr}|. \quad (5)$$

Here η_H is the mass accumulation efficiency for hydrogen burning. The values of η_H are

$$\eta_H = \begin{cases} \dot{M}_{cr}/|\dot{M}_{tr}|, & |\dot{M}_{tr}| > \dot{M}_{cr}, \\ 1, & \dot{M}_{cr} \geq |\dot{M}_{tr}| \geq \frac{1}{8}\dot{M}_{cr}, \\ 0, & |\dot{M}_{tr}| < \frac{1}{8}\dot{M}_{cr}. \end{cases} \quad (6)$$

When a certain amount of helium is accumulated, helium is assumed to be ignited. If He-shell flashes occur, then part of the helium is assumed to be blown off from the surface of the CO WD. η_{He} is the mass accumulation efficiency for He-shell flashes, and its value is taken from Kato & Hachisu (2004) (see also Meng et al. 2009). Note that the accumulation efficiencies used in this paper were derived for non-rotating WD models, but they are assumed to still be valid for rotating WDs (Wang et al. 2014). In addition, we assume that the mass lost as optically thick wind takes away the specific orbital angular momentum of the accreting WD, while the wind material which is not accreted by the WD carries off specific angular momentum of the secondary (Meng & Han 2016).

We consider a WD+RG scenario in the SD model and follow binary evolutions in which a WD accretes hydrogen-rich matter from its companion to increase its mass. For a rapidly rotating WD, we assume that the WD may continuously increase its mass when its mass exceeds the Chandrasekhar mass limit until the mass-transfer rate $|\dot{M}_{\text{tr}}|$ is lower than a critical mass-transfer rate \dot{M}_{ct} . Note that whether the accreting WDs are typically able to sustain differential rotation is theoretically uncertain, as is the \dot{M}_{ct} (Yoon & Langer 2004; Hachisu et al. 2012a,b; Wang et al. 2014). Therefore, for \dot{M}_{ct} , three different values are considered in our work: $1.0 \times 10^{-7} M_{\odot} \text{yr}^{-1}$, $3.0 \times 10^{-7} M_{\odot} \text{yr}^{-1}$ and $0.125 \dot{M}_{\text{cr}}$ (where \dot{M}_{cr} is the critical accretion rate of a WD, see Equation (3)). We record the WD mass at the point $|\dot{M}_{\text{tr}}| \leq \dot{M}_{\text{ct}}$ as the final mass of the WD exploding as the associated SN Ia. The initial masses of the CO WD M_{WD}^i are 0.8, 0.9, 1.0 and $1.1 M_{\odot}$, the initial orbital period $\log(P^i/d)$ is from 1.5 to 3.5 in steps of 0.1 and the companion masses range from $1.0 M_{\odot}$ to $4.5 M_{\odot}$ in steps of $0.1 M_{\odot}$.

3 RESULTS

We assume the WD can continuously increase mass when $M_{\text{WD}} > 1.378 M_{\odot}$ until the mass-transfer rate is lower than $1.0 \times 10^{-7} M_{\odot} \text{yr}^{-1}$. We give two representative examples of binary evolution calculations, as shown in Figures 1 and 2 respectively. In our calculations, the WD begins to increase its mass when the companion is on the asymptotic giant branch (AGB) (see Fig. 1) or red giant branch (RGB) (see Fig. 2).

In Figure 1, the initial binary parameters are $(M_2^i, M_{\text{WD}}^i, \log(P^i/d)) = (2.00 M_{\odot}, 1.00 M_{\odot}, 2.60)$. In this case, wind accretion becomes important at about 2×10^5 yr at which time the WD accretion rate is high enough to increase the WD mass. The donor star fills its Roche lobe after $\sim 10^5$ yr. The mass-transfer rate $|\dot{M}_{\text{tr}}|$

exceeds \dot{M}_{cr} soon after the start of RLOF, leading to a wind phase in which part of the transferred mass is blown off by the optically thick wind, and the rest is accumulated on the surface of the WD. After about 1.26×10^6 yr, $|\dot{M}_{\text{tr}}|$ drops below \dot{M}_{cr} but remains higher than $\frac{1}{2} \dot{M}_{\text{cr}}$. Thus, the optically thick wind stops and the hydrogen-shell burning is stable. The mass-transfer rate decreases further to below $\frac{1}{2} \dot{M}_{\text{cr}}$ but remains above $\frac{1}{8} \dot{M}_{\text{cr}}$, where hydrogen-shell burning is unstable, triggering very weak shell flashes, and the WD continues to grow in mass. The WD always grows in mass until the mass-transfer rate decreases to $1.0 \times 10^{-7} M_{\odot} \text{yr}^{-1}$. At this moment, the binary parameters are $(M_2^f, M_{\text{WD}}^f, \log(P^f/d)) = (0.5350 M_{\odot}, 1.4909 M_{\odot}, 3.1925)$. Another example of the initial binary system with $M_2^i = 1.40 M_{\odot}$, $M_{\text{WD}}^i = 1.10 M_{\odot}$ and $\log(P^i/d) = 2.00$ is shown in Figure 2. The binary evolves in a similar way as in the previous case and the final binary parameters are $M_2^f = 0.4084 M_{\odot}$, $M_{\text{WD}}^f = 1.5070 M_{\odot}$ and $\log(P^f/d) = 2.7657$ when the mass-transfer rate is lower than $1.0 \times 10^{-7} M_{\odot} \text{yr}^{-1}$. The main difference between this example and the previous one is that RLOF begins in the RGB stage, and that the system does not experience an optically thick wind phase and stable hydrogen-shell burning phase.

Figures 1(c) and 2(c) show the whole evolution of the secondary star on a Hertzsprung-Russell (HR) diagram, and the letters A, B, ... and F indicate the positions of the companion star at different spin-down timescales. We list some essential properties of the companion corresponding to these positions in Tables 1 and 2. If t is defined as the timescale between the time of the end of the mass growth of the WD and the time that the companion star's luminosity is below the current detection limit, from Figures 1(c) and 2(c), we can see that t is around 10^7 yr. This timescale is consistent with the estimation by Meng & Podsiadlowski (2013). Thus, if we assume that the spin-down timescale is a few 10^7 yr, the companion is most likely too dim to be detected.

Figure 3 shows the final WD and companion masses at the moment when the WD stops increasing its mass with different initial WD masses. The final WD mass ranges from $1.378 M_{\odot}$ to $2.707 M_{\odot}$. For $M_{\text{WD}}^i = 0.8 M_{\odot}$ and $0.9 M_{\odot}$, the companions are all RG stars at the moment when the WD stops increasing its mass. However, the companions may be either AGB or RGB stars for $M_{\text{WD}}^i = 1.0 M_{\odot}$ and $1.1 M_{\odot}$, and the masses of those AGB stars are larger than $0.5 M_{\odot}$. Before the WD explodes as an SN Ia, the companion will continue to evolve and become a CO or He WD for a long spin-down timescale of the WD. The evolution of the com-

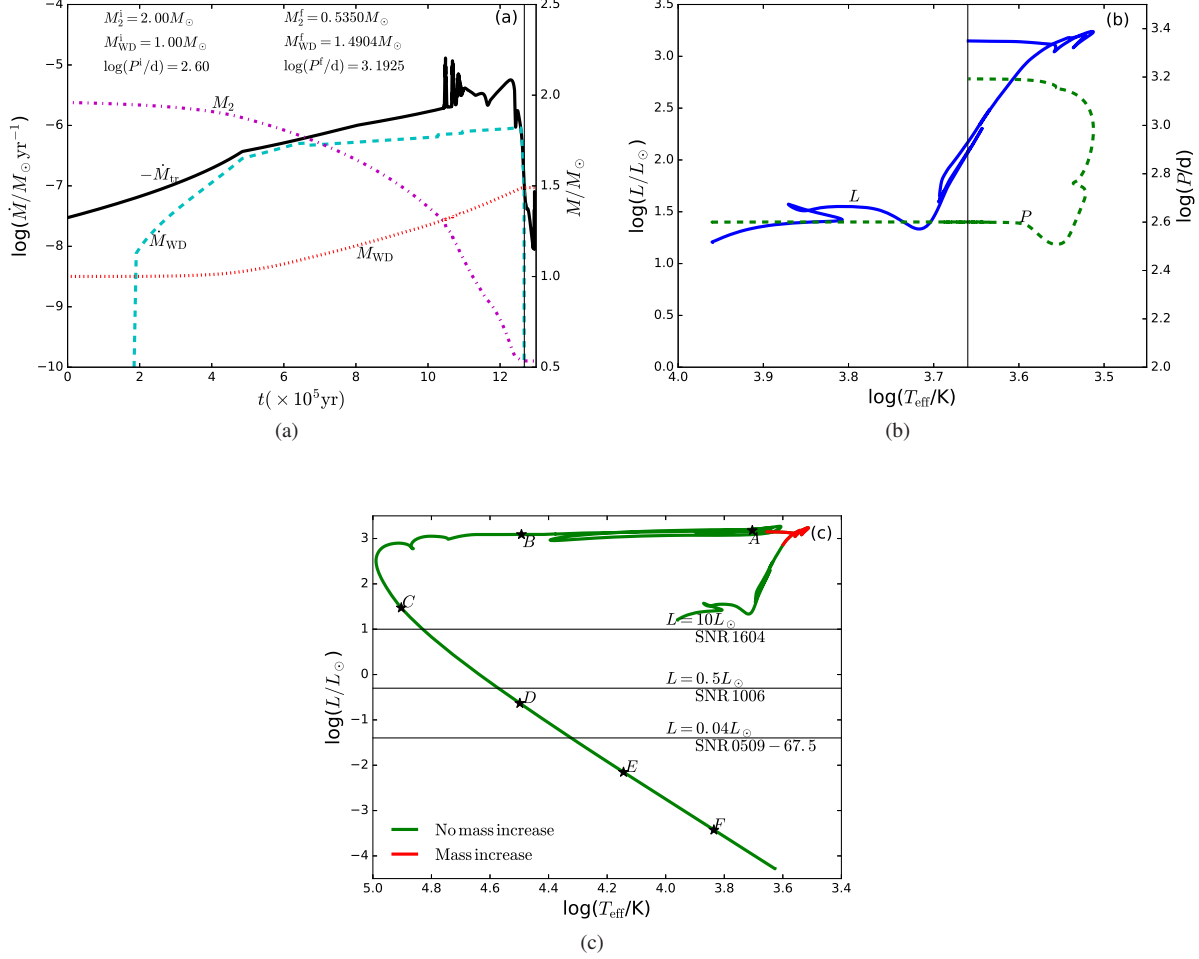


Fig. 1 An example of binary evolution calculations. Panel (a): evolutions of the mass-transfer rate $-\dot{M}_{\text{tr}}$, the mass-growth rate of the CO WD \dot{M}_{WD} , the secondary mass M_2 and the CO WD mass M_{WD} as a function of time. Time is offset by 1.519×10^9 yr from the birth of the system. The initial binary parameters and parameters at the time when the WD stops increasing its mass are also shown. Panel (b): evolutions of the luminosity of the secondary star (*solid curve*) and binary orbital period (*dashed curve*) are shown. The vertical lines in both panels indicate the position where the WD stops increasing its mass. Panel (c): HR diagram of the secondary star. The red line indicates the phase in which the mass of the WD is growing. The letters A, B, and F indicate the positions of the companion star at spin-down time of 10^4 yr, 10^5 yr, . . . and 10^9 yr respectively. The luminosities of $L = 10 L_\odot$, $L = 0.5 L_\odot$ and $L = 0.04 L_\odot$ in this panel represent detection limits for different SN Ia remnants.

Table 1 Some Properties of the Companion with $M_2^i = 2.00 M_\odot$ (see also Fig. 1)

Stage	Spin-down time (yr)	$M_2 (M_\odot)$	$\log L (L_\odot)$	$\log T_{\text{eff}} (\text{K})$	$\log P (\text{d})$	$v_{\text{orb}} (\text{km s}^{-1})$
A	10^4	0.534	3.18	3.70	3.194	23.22
B	10^5	0.533	3.09	4.50	3.196	23.17
C	10^6	0.533	1.46	4.90	3.196	23.17
D	10^7	0.533	-0.63	4.50	3.196	23.17
E	10^8	0.533	-2.15	4.15	3.196	23.17
F	10^9	0.533	-3.43	3.83	3.196	23.17

panion star in the HR diagram with different spin-down times is shown in Figure 4. Regardless of the interaction between SN ejecta and the companion, from this figure, we can see that if the spin-down time is short enough

(e.g. $< 10^6$ yr), the secondary star will be very bright and easily observed. However, if the spin-down timescale is longer than $\sim 10^7$ yr, the luminosities of these companions will be dimmer than the current detection lim-

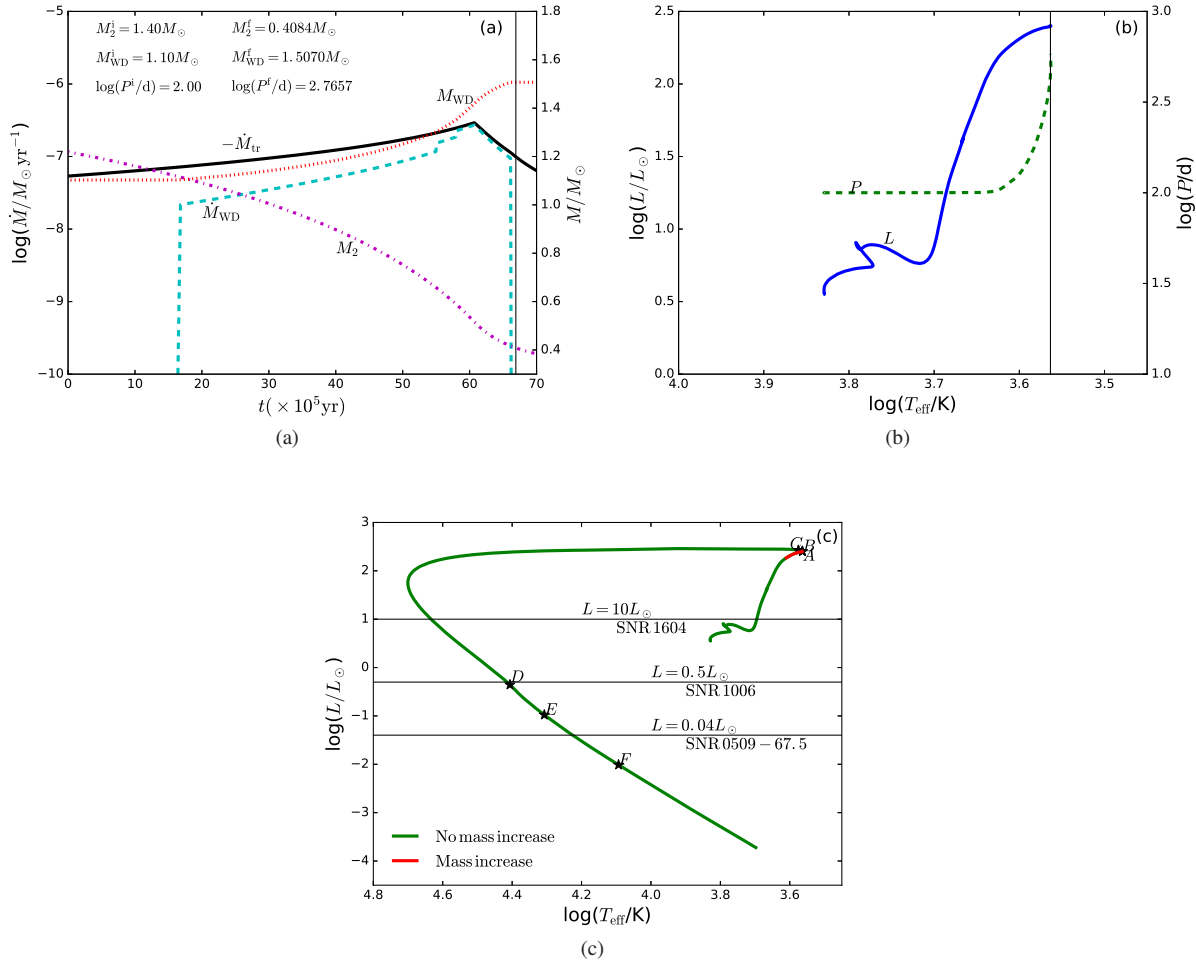


Fig. 2 Another typical example of binary evolution calculations. Similar to Fig. 1, but the time is offset by 3.704×10^9 yr so that the timescale for the accretion process is more easily seen in this figure. The companion is an RG star when the WD begins to increase its mass by accretion.

Table 2 Some Properties of the Companion with $M_2^i = 1.40 M_{\odot}$ (see also Fig. 2)

Stage	Spin-down time (yr)	M_2 (M_{\odot})	$\log L$ (L_{\odot})	$\log T_{\text{eff}}$ (K)	$\log P$ (d)	v_{orb} (km s^{-1})
A	10^4	0.407	2.40	3.56	2.770	31.54
B	10^5	0.399	2.41	3.56	2.793	30.94
C	10^6	0.353	2.43	3.58	2.934	27.55
D	10^7	0.334	-0.36	4.41	2.997	26.16
E	10^8	0.334	-0.98	4.31	2.997	26.16
F	10^9	0.334	-2.01	4.09	2.997	26.16

its. This may explain the difficulty in finding a surviving companion. In addition, because the stellar evolution time from the AGB stage or RGB stage across the planetary nebula stage to the WD cooling track is fairly short, and the exact position of the companion in the HR diagram for a different spin-down timescale is heavily dependent on the hydrogen mass on top of the core of the companion at the moment that the WD stops increasing its mass, points corresponding to $\tau_{\text{SD}} = 10^4, 10^5$

and 10^6 yr are relatively scattered. However, points corresponding to $\tau_{\text{SD}} = 10^7, 10^8$ and 10^9 yr are relatively concentrated, which is mainly because at these times almost all companions are WDs, and their masses and chemical compositions are almost no longer changed. Two cooling tracks obviously appear in the figure; one cooling sequence represents CO WDs and the other represents He WDs.

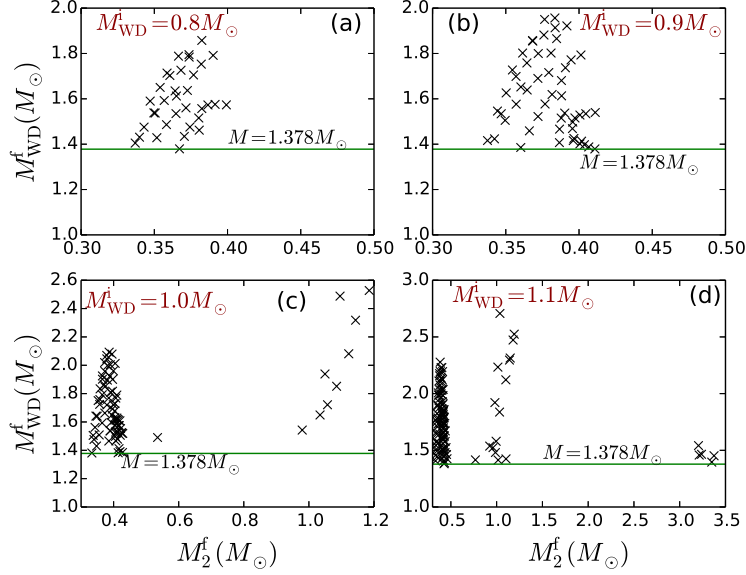


Fig. 3 The final WD and companion masses for different initial WD masses, where M_2^i and M_{WD}^f are the masses of the companion star and WD when the WD cannot grow in mass anymore. “x” symbols indicate systems resulting in SN Ia explosions.

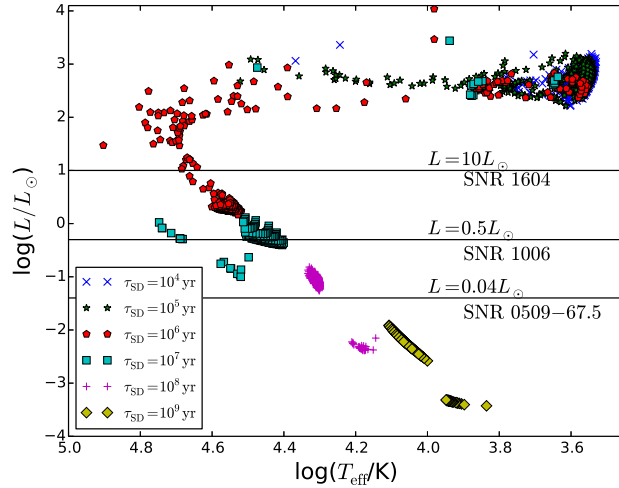


Fig. 4 HR diagram of companion stars. τ_{SD} indicates the spin-down time, i.e. the time between the end of the mass growth of the WD and the explosion. The luminosities of $L = 10 L_{\odot}$, $L = 0.5 L_{\odot}$ and $L = 0.04 L_{\odot}$ in the figure denote the current detection limits for different SN Ia remnants. Six spin-down times are represented by different colors and symbols, as shown in the figure.

Figure 5 shows the final WD mass M_{WD}^f versus the initial secondary mass M_2^i for various sets of parameters, M_{WD}^i and \dot{M}_{ct} , where $\log(P^i/d) = 2.50$. We can see from the figure that the less massive the companion, the more significant the difference between the final WD masses for different \dot{M}_{ct} , especially for $\dot{M}_{\text{ct}} = 0.125 \dot{M}_{\text{cr}}$ and $3.0 \times 10^{-7} M_{\odot} \text{ yr}^{-1}$. \dot{M}_{cr} is a function of WD mass and $0.125 \dot{M}_{\text{cr}}$ increases with the increase of WD mass to close to the value of $3.0 \times 10^{-7} M_{\odot} \text{ yr}^{-1}$. For a given binary system with a less massive com-

panion, the WD may increase its mass to a relatively smaller value, which means that the difference between $0.125 \dot{M}_{\text{cr}}$ and $3.0 \times 10^{-7} M_{\odot} \text{ yr}^{-1}$ is more significant. Therefore, the WD stops increasing its mass earlier for the choice $\dot{M}_{\text{ct}} = 3.0 \times 10^{-7} M_{\odot} \text{ yr}^{-1}$ than for the choice $\dot{M}_{\text{ct}} = 0.125 \dot{M}_{\text{cr}}$, i.e. the final mass of the WD for $\dot{M}_{\text{ct}} = 0.125 \dot{M}_{\text{cr}}$ is larger than that for $\dot{M}_{\text{ct}} = 3.0 \times 10^{-7} M_{\odot} \text{ yr}^{-1}$. However, the maximum difference between the final WD mass for different \dot{M}_{ct} is only

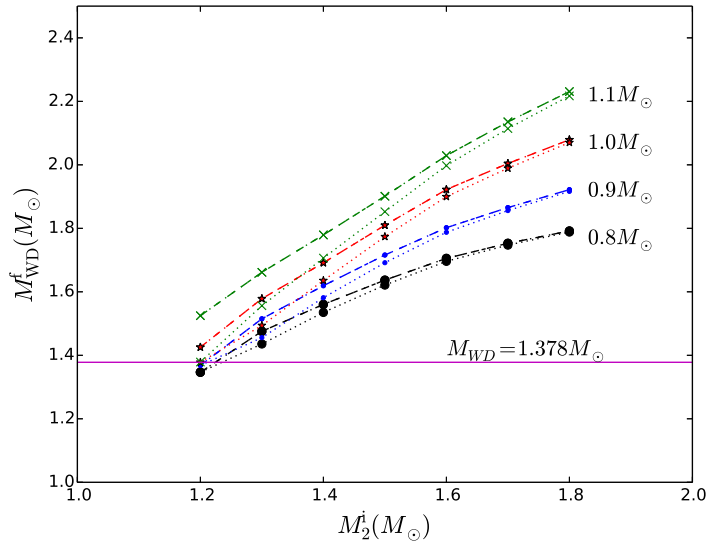


Fig. 5 The final WD masses versus the initial secondary masses for different \dot{M}_{ct} and M_{WD}^i . $M_{\text{WD}}^f(M_{\odot})$ represents the WD mass at the moment that the WD stops increasing its mass when the mass-transfer rate decreases to \dot{M}_{ct} . Dashed, dash-dotted and dotted lines indicate the cases of $\dot{M}_{\text{ct}} = 1.0 \times 10^{-7} M_{\odot} \text{ yr}^{-1}$, $0.125 \dot{M}_{\text{cr}}$ and $3.0 \times 10^{-7} M_{\odot} \text{ yr}^{-1}$ respectively. Four sequences represent different M_{WD}^i as shown in the figure.

$0.106 M_{\odot}$, i.e. the different choices of \dot{M}_{ct} may not significantly influence the main results.

4 DISCUSSION

Tables 1 and 2 show some essential properties of the companion star with different spin-down times. With the evolution of the companion, its luminosity and mass as well as its orbital velocity are becoming smaller.

In Figure 6, we plot the evolution of the distributions of binary system parameters with the spin-down time τ_{SD} . For simplicity, we only show the case of $M_{\text{WD}}^i = 1.10 M_{\odot}$, and the results for other initial WD masses are similar. A small number of companions with $M_2^i > 0.5 M_{\odot}$ in Figure 3(d) are displayed in Figure 6(b). From the figure, we can see that if the spin-down time is long enough, signatures thought to be indispensable parts of the SD model are diminished. For example, many companion stars will have lost their envelopes prior to explosion if the spin-down timescale is long enough, and the binary will have a lower orbital velocity, which is consistent with the suggestion from Di Stefano et al. (2011). In addition, the mass of the companion can be as low as $\sim 0.3 M_{\odot}$ for a long spin-down timescale, which conforms to the suggestion that the surviving companions of old SNe Ia from the WD+RG channel have a low mass (see also Wang & Han 2010a; Meng & Yang 2010; Justham et al. 2009). Thus, this provides a possible way to explain the formation of the population of single low-mass WDs ($< 0.45 M_{\odot}$).

Additionally, a spin-down time of $\sim 10^7$ yr allows most companions to be WDs, and thus these companions may tend to be dim (as shown in Fig. 4), i.e. it will be difficult to detect such companions. A survey from González Hernández et al. (2012) and Kerzendorf et al. (2012) which aims to find the surviving companion of the SN 1006 progenitor indicated that SN 1006 probably follows the DD model, because no subgiant or giant companion star has been found in SNR 1006. Moreover, González Hernández et al. (2012) demonstrate that current models do not support long timescales for angular momentum redistribution and loss, and the upper limit on the timescale for angular momentum redistribution and loss seems to be only $\sim 10^6$ yr. The spin-down time in the WD is mainly determined by the timescale for angular momentum redistribution or loss. However, the timescale for angular momentum redistribution or loss is theoretically uncertain, leading to an uncertainty in spin-down time. Based on the result here, if the spin-down timescale is as long as $\sim 10^7$ yr, the companion may be too dim to be detected. Such a timescale is consistent with the estimation in Meng & Podsiadlowski (2013). Hence the fact that no surviving companion in SNR 1006 has been observed does not mean that SN 1006 definitely comes from the DD model.

At present, the critical mass-transfer rate \dot{M}_{ct} is still uncertain. In this paper, in order to examine the effect of critical mass-transfer rate \dot{M}_{ct} on the final results, we adopt three values used in the literature.

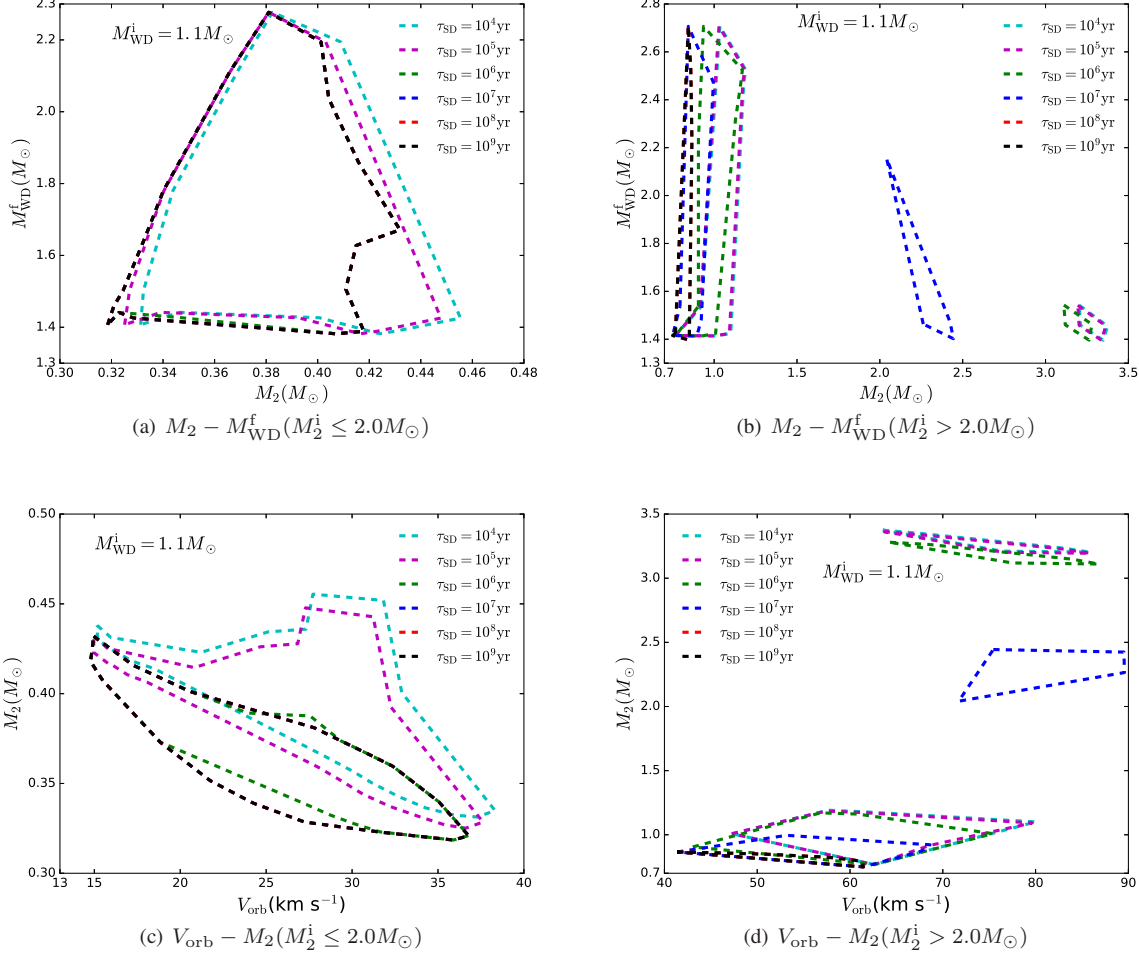


Fig. 6 Companion stars in the planes of (M_2, M_{WD}^f) and (V_{orb}, M_2) , where $M_{WD}^i = 1.1 M_{\odot}$, $\dot{M}_{ct} = 1.0 \times 10^{-7} M_{\odot} \text{ yr}^{-1}$. M_2 , M_{WD}^f and V_{orb} are the companion mass, the WD mass and the orbital velocity at different spin-down timescales (τ_{SD}) respectively. Panels (a) and (c): the initial companion mass M_2^i ranges from $1.0 M_{\odot}$ to $2.0 M_{\odot}$ and these companion stars eventually evolve into He WDs. Panels (b) and (d): the initial companion mass M_2^i is larger than $2.0 M_{\odot}$ and these companion stars eventually evolve into CO WDs. Both V_{orb} and M_2 significantly decrease with the spin-down time.

In Figure 7, we show the binary system parameters at $\tau_{SD} = 10^7$ yr for different \dot{M}_{ct} . We can see that the smaller the \dot{M}_{ct} , the lower the final mass of the companion, i.e., the companion may have a thinner envelope for a lower \dot{M}_{ct} and so it may take a shorter time from RGB or AGB stage to WD cooling track, causing the difference in t . However, the influence of the different choice for \dot{M}_{ct} on t is very small and t is around 10^7 yr for different \dot{M}_{ct} . Furthermore, it has been shown that the WDs have larger final masses for a lower \dot{M}_{ct} , but the effect of different \dot{M}_{ct} on the final orbital parameters of the binary system is not significant.

Generally, if $M_{WD}^f < 1.48 M_{\odot}$, the rotation of the WD is rigid, but for a more massive WD, the rotation will become differential. Hachisu et al. (2012a) discussed

this issue and showed that the spin-down time in the mid-mass range ($1.5 M_{\odot} < M_{WD} < 2.4 M_{\odot}$) WDs was $\sim 10^8$ yr due to angular momentum redistribution or loss by the Eddington-Sweet meridional circulation (see also Yoon & Langer 2004), and in lower mass range ($1.38 M_{\odot} < M_{WD} < 1.5 M_{\odot}$) WDs was $\sim 10^9$ yr determined by angular momentum loss by the magnetodipole radiation. Moreover, in the extremely massive case, the WDs which are supported by differential rotation explode as SNe Ia soon after the WD masses exceed $2.4 M_{\odot}$ owing to a secular instability. This is not the common case. Here, we select models with $M_{WD}^f < 1.48 M_{\odot}$ and exhibit the evolution of companion stars for these models with τ_{SD} , as shown in Figure 8. t is still approximately $\sim 10^7$ yr which is much shorter than

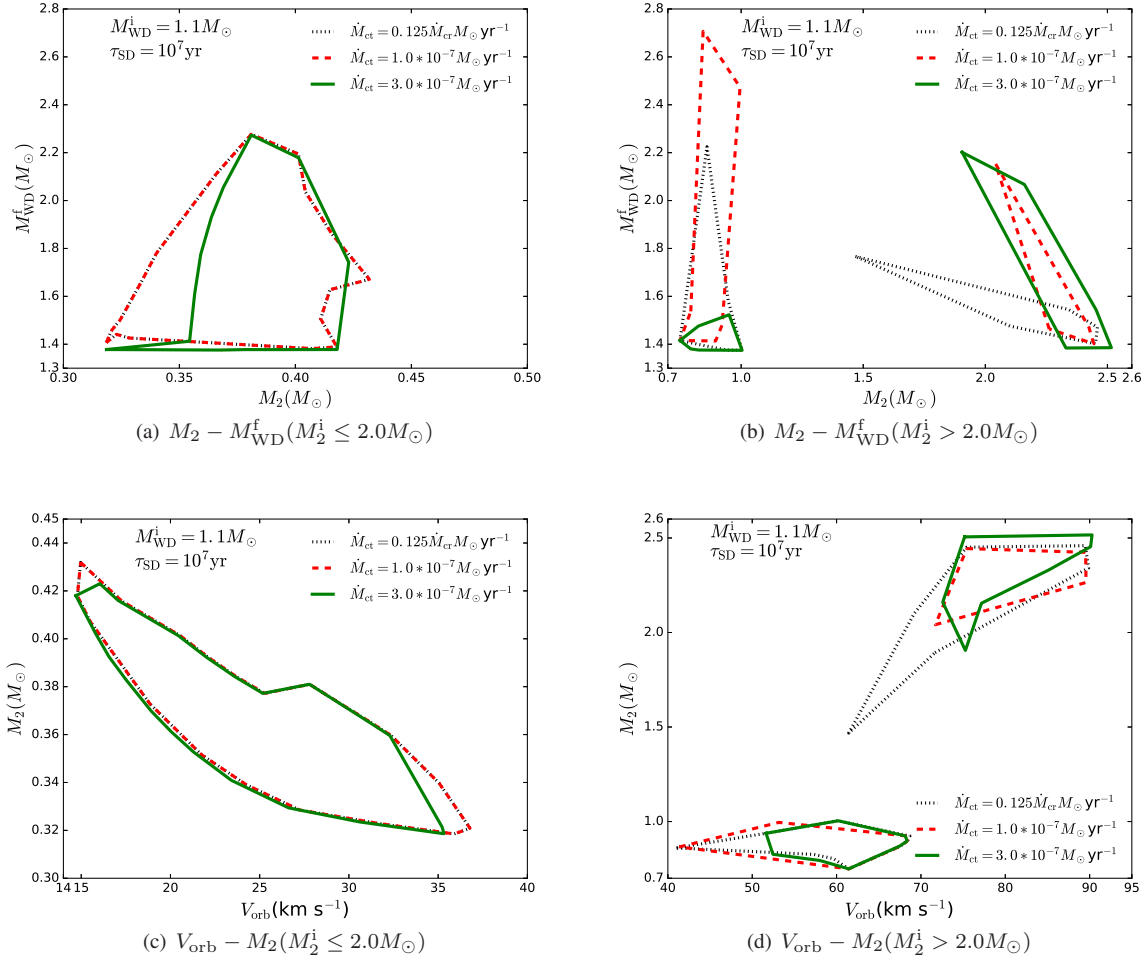


Fig. 7 Similar to Fig. 6, but for different \dot{M}_{ct} ($\tau_{\text{SD}} = 10^7$ yr).

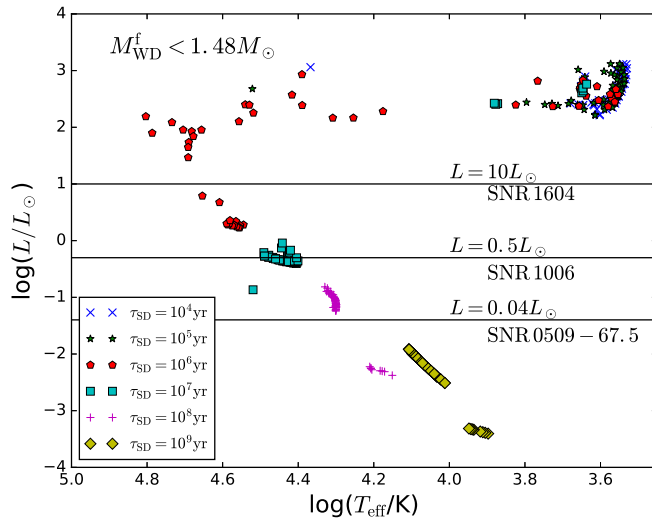


Fig. 8 Like Fig. 4, but only for models with $M_{\text{WD}}^f < 1.48 M_{\odot}$.

$\sim 10^9$ yr adopted in Hachisu et al. (2012a). Therefore, if the final mass of the WD is lower than $1.48 M_{\odot}$, it is very likely that the companion cannot be discovered.

Similarly, the spin-down timescale is also related to the initial masses of the WDs. Wang et al. (2014) studied the evolution of rotating accreting WDs and showed the following results:

- (1) For the initial WD mass of 0.657, 0.70 and $0.75 M_{\odot}$, the WD exploded as an SN Ia with WD mass in the range $1.378 \leq M_{\text{WD}} < 1.5 M_{\odot}$, which can be supported by solid-body rotation.
- (2) If the initial WD mass is 0.8 and $0.9 M_{\odot}$, the WD would explode as an SN Ia with the WD mass in the range $1.378 \leq M_{\text{WD}} < 1.5 M_{\odot}$ and $1.5 < M_{\text{WD}} < 2.0 M_{\odot}$ respectively.
- (3) While for the initial WD mass of 1.0, 1.1 and $1.2 M_{\odot}$, the WD would explode as an SN Ia with WD mass in the range $1.378 \leq M_{\text{WD}} < 1.5 M_{\odot}$, $1.5 < M_{\text{WD}} < 2.0 M_{\odot}$ and $M_{\text{WD}} \geq 2.0 M_{\odot}$. However, the explosion mass of the WD exceeds $2.4 M_{\odot}$ only when $M_{\text{WD}}^i \geq 1.2 M_{\odot}$ respectively.

Therefore, in conjunction with the previous discussion, we can find the relationship between spin-down timescale and initial mass of the WD. Furthermore, Wang et al. (2014) presented a detailed binary population synthesis study to examine the predicted population of SNe Ia. The results of the simulation showed that 77 per cent of these exploding WDs are predicted to have masses in the range $1.378 \leq M_{\text{WD}} < 1.5 M_{\odot}$, corresponding to normal SNe Ia and 91bg-like events (see also Hachisu et al. 2012a); only 2 per cent of the total have WD explosion masses $\geq 2.0 M_{\odot}$. Thus, overluminous SNe Ia could be relatively rare, and the majority of SNe Ia in the observations should be normal SNe Ia. According to the recorded brightness and spectra, the peak magnitude of SN 1572 was around -4.0 , consistent with a normal SN Ia in terms of luminosity, and Kepler’s observed peak magnitude was $m \sim -3.0$ (i.e. $M_v \simeq -18.8$). It is also a typically normal SN Ia. This result does not contradict the assumptions in this paper, that is, the exploding WD rotates very fast and finally explodes at a mass exceeding M_{Ch} , and the resulting SN Ia is not necessarily very bright.

5 SUMMARY AND CONCLUSIONS

We carry out binary evolution calculations for the WD+RG channel by assuming that a mass-accreting, stably rotating WD may continuously increase its mass when its mass exceeds the Chandrasekhar mass limit

until the mass transfer rate is lower than a critical mass-transfer rate \dot{M}_{ct} ($\dot{M}_{\text{ct}} = 0.125 \dot{M}_{\text{cr}}, 1.0 \times 10^{-7} M_{\odot} \text{yr}^{-1}$ or $3.0 \times 10^{-7} M_{\odot} \text{yr}^{-1}$). Our main results can be summarized as follows:

- (1) The final WDs have a mass ranging from $1.378 M_{\odot}$ to $2.707 M_{\odot}$ depending on the critical mass-transfer rate, and the companion will become a CO or He WD if the spin-down timescale is long enough.
- (2) The timescale t between the time of the end of mass growth for the WD and the time that the companion star’s luminosity is below the current detection limit is approximately a few 10^7 yr, consistent with the estimation in Meng & Podsiadlowski (2013). When t is a few 10^7 yr, the companions tend to be dim. Hence, the surviving companions are difficult to be detected, which is a possible explanation for the fact that no expected surviving companion has been discovered in Kepler’s SNR (Kerzendorf et al. 2014) or SNR 1006 (Kerzendorf et al. 2012; González Hernández et al. 2012).
- (3) In this paper, we adopt three different critical rates, \dot{M}_{ct} , and we show that the higher the critical rate \dot{M}_{ct} , the lower the final WD masses and the higher the final companion masses. However, the different choice of critical mass-transfer rate \dot{M}_{ct} may not significantly affect our main conclusion.

Acknowledgements We are grateful to the anonymous referee for his or her useful comments and suggestions. This work was partly supported by NSFC (11522327, 11473036, 11521303 and 11390374), CAS “Light of West China” Program, CAS (No. KJZD-EW-M06-01) and the Science and Technology Innovation Talent Program of Yunnan Province (Grant No. 2013HA005).

References

- Alexander, D. R., & Ferguson, J. W. 1994, ApJ, 437, 879
 Boffin, H. M. J., & Jorissen, A. 1988, A&A, 205, 155
 Burkey, M. T., Reynolds, S. P., Borkowski, K. J., & Blondin, J. M. 2013, ApJ, 764, 63
 Chen, W.-C., & Li, X.-D. 2007, ApJ, 658, L51
 Chen, W.-C., & Li, X.-D. 2009, ApJ, 702, 686
 Chen, X., Han, Z., & Tout, C. A. 2011, ApJ, 735, L31
 Chen, X.-F., & Tout, C. A. 2007, ChJAA (Chin. J. Astron. Astrophys.), 7, 245
 Chiotellis, A., Kosenko, D., Schure, K. M., & Vink, J. 2013, in IAU Symposium, 281, Binary Paths to Type Ia Supernovae Explosions, eds. R. Di Stefano, M. Orio, & M. Moe, 331
 Chiotellis, A., Schure, K. M., & Vink, J. 2012, A&A, 537, A139
 Di Stefano, R., Voss, R., & Claeys, J. S. W. 2011, ApJ, 738, L1

- Eggleton, P. P. 1971, *MNRAS*, 151, 351
- Eggleton, P. P. 1972, *MNRAS*, 156, 361
- Eggleton, P. P. 1973, *MNRAS*, 163, 279
- González Hernández, J. I., Ruiz-Lapuente, P., Filippenko, A. V., et al. 2009, *ApJ*, 691, 1
- González Hernández, J. I., Ruiz-Lapuente, P., Tabernero, H. M., et al. 2012, *Nature*, 489, 533
- González-Hernández, J. I., Ruiz-Lapuente, P., Tabernero, H. M., et al. 2015, in *Highlights of Spanish Astrophysics VIII*, eds. A. J. Cenarro, F. Figueras, C. Hernández-Monteagudo, J. Trujillo Bueno, & L. Valdivielso, 488
- Greggio, L., & Renzini, A. 1983, *A&A*, 118, 217
- Hachisu, I., Kato, M., & Nomoto, K. 1996, *ApJ*, 470, L97
- Hachisu, I., Kato, M., & Nomoto, K. 1999a, *ApJ*, 522, 487
- Hachisu, I., Kato, M., & Nomoto, K. 2012a, *ApJ*, 756, L4
- Hachisu, I., Kato, M., Nomoto, K., & Umeda, H. 1999b, *ApJ*, 519, 314
- Hachisu, I., Kato, M., Saio, H., & Nomoto, K. 2012b, *ApJ*, 744, 69
- Han, Z., & Podsiadlowski, P. 2004, *MNRAS*, 350, 1301
- Han, Z., Podsiadlowski, P., & Eggleton, P. P. 1994, *MNRAS*, 270, 121
- Han, Z., Tout, C. A., & Eggleton, P. P. 2000, *MNRAS*, 319, 215
- Iben, Jr., I., & Tutukov, A. V. 1984, *ApJS*, 54, 335
- Iglesias, C. A., & Rogers, F. J. 1996, *ApJ*, 464, 943
- Justham, S. 2011, *ApJ*, 730, L34
- Justham, S., Wolf, C., Podsiadlowski, P., & Han, Z. 2009, *A&A*, 493, 1081
- Kato, M., & Hachisu, I. 2004, *ApJ*, 613, L129
- Kerzendorf, W. E., Childress, M., Scharwächter, J., Do, T., & Schmidt, B. P. 2014, *ApJ*, 782, 27
- Kerzendorf, W. E., Schmidt, B. P., Laird, J. B., Podsiadlowski, P., & Bessell, M. S. 2012, *ApJ*, 759, 7
- Kerzendorf, W. E., Yong, D., Schmidt, B. P., et al. 2013, *ApJ*, 774, 99
- Langer, N., Deutschmann, A., Wellstein, S., & Höflich, P. 2000, *A&A*, 362, 1046
- Li, X.-D., & van den Heuvel, E. P. J. 1997, *A&A*, 322, L9
- Lindblom, L. 1999, *Phys. Rev. D*, 60, 064007
- Matteucci, F., & Greggio, L. 1986, *A&A*, 154, 279
- Meng, X., Chen, X., & Han, Z. 2009, *MNRAS*, 395, 2103
- Meng, X., Gao, Y., & Han, Z. 2015, *International Journal of Modern Physics D*, 24, 1530029
- Meng, X., & Han, Z. 2016, *A&A*, 588, A88
- Meng, X., & Podsiadlowski, P. 2013, *ApJ*, 778, L35
- Meng, X., & Yang, W. 2010, *A&A*, 516, A47
- Nomoto, K. 1982, *ApJ*, 253, 798
- Nomoto, K., Iwamoto, K., & Kishimoto, N. 1997, *Science*, 276, 1378
- Pan, K.-C., Ricker, P. M., & Taam, R. E. 2014, *ApJ*, 792, 71
- Patnaude, D. J., Badenes, C., Park, S., & Laming, J. M. 2012, *ApJ*, 756, 6
- Perlmutter, S., Aldering, G., Goldhaber, G., et al. 1999, *ApJ*, 517, 565
- Pols, O. R., Schröder, K.-P., Hurley, J. R., Tout, C. A., & Eggleton, P. P. 1998, *MNRAS*, 298, 525
- Pols, O. R., Tout, C. A., Eggleton, P. P., & Han, Z. 1995, *MNRAS*, 274, 964
- Pols, O. R., Tout, C. A., Schroder, K.-P., Eggleton, P. P., & Manners, J. 1997, *MNRAS*, 289, 869
- Reimers, D. 1975, *Memoires of the Societe Royale des Sciences de Liege*, 8, 369
- Riess, A. G., Filippenko, A. V., Challis, P., et al. 1998, *AJ*, 116, 1009
- Ruiz-Lapuente, P., Comeron, F., Méndez, J., et al. 2004, *Nature*, 431, 1069
- Schroder, K.-P., Pols, O. R., & Eggleton, P. P. 1997, *MNRAS*, 285, 696
- Tout, C. A., & Eggleton, P. P. 1988, *MNRAS*, 231, 823
- Wang, B., & Han, Z. 2009, *A&A*, 508, L27
- Wang, B., & Han, Z. 2010a, *MNRAS*, 404, L84
- Wang, B., & Han, Z. 2012, *New Astron. Rev.*, 56, 122
- Wang, B., & Han, Z.-W. 2010b, *RAA (Research in Astronomy and Astrophysics)*, 10, 235
- Wang, B., Justham, S., Liu, Z.-W., et al. 2014, *MNRAS*, 445, 2340
- Webbink, R. F. 1984, *ApJ*, 277, 355
- Yoon, S.-C., & Langer, N. 2004, *A&A*, 419, 623
- Yoon, S.-C., & Langer, N. 2005, *A&A*, 435, 967